Title

Identifying Toxicologically Significant Compounds in Urban Wildfire Ash Using In Vitro Bioassays and High-Resolution Mass Spectrometry

Journal

Environmental Science and Technology, 55(6)

ISSN

0013-936X

Authors

Young, Thomas M
Black, Gabrielle P
Wong, Luann
et al.

Publication Date

2021-03-16

DOI

10.1021/acs.est.0c06712

Peer reviewed

HHS Public Access

Author manuscript

Environ Sci Technol. Author manuscript; available in PMC 2021 August 09.

Published in final edited form as:

Environ Sci Technol. 2021 March 16; 55(6): 3657–3667. doi:10.1021/acs.est.0c06712.

Identifying Toxicologically Significant Compounds in Urban Wildfire Ash Using *In vitro* Bioassays and High-Resolution Mass Spectrometry

Thomas M. Young,
Department of Civil & Environmental Engineering and Agricultural and Environmental Chemistry Graduate Group, University of California, Davis, Davis, California 95616, United States

Gabrielle P. Black,
Department of Civil & Environmental Engineering and Agricultural and Environmental Chemistry Graduate Group, University of California, Davis, Davis, California 95616, United States

Luann Wong,
Department of Civil & Environmental Engineering, University of California, Davis, Davis, California 95616, United States

Clayton S. Bloszies,
Agricultural and Environmental Chemistry Graduate Group and West Coast Metabolomics Center, University of California, Davis, Davis, California 95616, United States

Oliver Fiehn,
Agricultural and Environmental Chemistry Graduate Group and West Coast Metabolomics Center, University of California, Davis, Davis, California 95616, United States

Guochun He,
Department of Environmental Toxicology, University of California, Davis, Davis, California 95616, United States

Michael S. Denison,
Department of Environmental Toxicology, University of California, Davis, Davis, California 95616, United States

Corresponding Author Thomas M. Young – Department of Civil & Environmental Engineering and Agricultural and Environmental Chemistry Graduate Group, University of California, Davis, Davis, California 95616, United States, Phone: 530-754-9399, tyoung@ucdavis.edu.

ASSOCIATED CONTENT

Supporting Information

The Supporting Information is available free of charge at https://pubs.acs.org/doi/10.1021/acs.est.0c06712.

Sampling location GPS; LC internal standards; retention index calculation procedure; description of nontarget workflow parameter selection and performance; optimized parameter settings for GC and LC alignment using MS-DIAL; GC target compound results and relation to nontarget peak areas; results of optimized workflows for target compounds; and complete summaries of alignment results for GC EI, LC ESI$^+$, and LC ESI$^-$ (XLSX)

Complete lists of statistically significant relationships between the aligned features on each instrument platform and all bioassay results; CALUX AhR results for pure compounds selected for relationship to AhR activity in wildfire ash extracts; results of ER and AR antagonism tests for wildfire extracts; macrophage cell viability test results; tentative identification, structure, and mass spectra of GC–EI features statistically related to bioassay activity; and MS-FINDER annotations for selected MS/MS spectra of features related to bioassay activity (PDF)

Complete contact information is available at: https://pubs.acs.org/10.1021/acs.est.0c06712

The authors declare no competing financial interest.

Christoph F.A. Vogel,
Department of Environmental oxicology and Center for Health and the Environment, University of California, Davis, Davis, California 95616, United States

Blythe Durbin-Johnson
Division of Biostatistics, School of Medicine, University of California, Davis, Davis, California 95616, United States

Abstract

Urban wildfires may generate numerous unidentified chemicals of toxicity concern. Ash samples were collected from burned residences and from an undeveloped upwind reference site, following the Tubbs fire in Sonoma County, California. The solvent extracts of ash samples were analyzed using GC– and LC– high-resolution mass spectrometry (HRMS) and using a suite of *in vitro* bioassays for their bioactivity toward nuclear receptors [aryl hydrocarbon receptor (AhR), estrogen receptor (ER), and androgen receptor (AR)], their influence on the expression of genetic markers of stress and inflammation [interleukin-8 (IL-8) and cyclooxygenase-2 (COX-2)], and xenobiotic metabolism [cytochrome P4501A1 (CYP1A1)]. Genetic markers (CYP1A1, IL-8, and COX-2) and AhR activity were significantly higher with wildfire samples than in solvent controls, whereas AR and ER activities generally were unaffected or reduced. The bioassay responses of samples from residential areas were not significantly different from the samples from the reference site despite differing chemical compositions. Suspect and nontarget screening was conducted to identify the chemicals responsible for elevated bioactivity using the multiple streams of HRMS data and open-source data analysis workflows. For the bioassay endpoint with the largest available database of pure compound results (AhR), nontarget features statistically related to whole sample bioassay response using Spearman's rank-order correlation coefficients or elastic net regression were significantly more likely (by 10 and 15 times, respectively) to be known AhR agonists than the overall population of compounds tentatively identified by nontarget analysis. The findings suggest that a combination of nontarget analysis, *in vitro* bioassays, and statistical analysis can identify bioactive compounds in complex mixtures.

Graphical Abstract

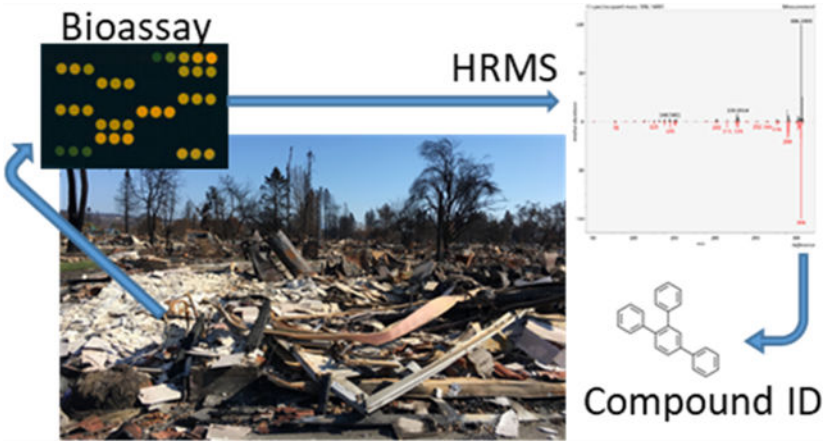

INTRODUCTION

The size and destructiveness of wildfires has increased during recent years. For example, in the state of California, nine of the ten largest and three of the five deadliest wildfires since 1932 have occurred since 2012, and the West Coast of the United States is presently in the midst of another record-setting wildfire season.[1] In part, the increase in deaths and property damage caused by wildfires is because the fires are occurring nearer to developed areas. Following the critical and immediate danger to life and human health caused by the fires and associated air pollution, important questions remain related to human health and environmental effects in residential areas in the aftermath of urban wildfires.

Wildfire smoke contains numerous chemicals of health concern, with polycyclic aromatic hydrocarbons (PAHs) and polychlorinated dibenzo-*p*-dioxins and dibenzofurans (dioxin-like chemicals) chief among them.[2–4] Residual contamination remains after the fires; concentrations of PAHs, for example, are typically elevated in soils following fires.[5] Wildfires in residential areas have the potential to produce a variety of combustion byproducts beyond PAHs and dioxins because of the complex chemistry of the household construction materials and home contents. Synthetic materials (e.g., polymers, adhesives, coatings, and pesticides) are widespread in modern homes, and these materials may produce novel combustion byproducts that can impact human health during and after wildfires.[6] Hazardous materials remaining in ash or soil after wildfires may affect the safety of reconstruction activities, home gardens and their produce, water supplies, and outdoor recreation within burned areas.

Nontarget chemical analysis using liquid and/or gas chromatography with high-resolution mass spectrometry (HRMS) has greatly expanded the list of chemicals that can be detected in environmental samples.[7,8] These techniques are particularly useful for detecting and identifying reaction byproducts, which may not have been purposely synthesized previously and therefore may be missing from chemical databases.[9] Environmental applications of nontarget analysis have generally employed LC–HRMS methods and workflows.[10] The soft ionization techniques typically employed in LC–HRMS such as electrospray ionization (ESI) produce quasi-molecular ions (e.g., $[M + H]^+$ or $[M – H]^–$), facilitating the alignment of features using retention time and molecular ion mass-to-charge ratio. Environmental applications of nontarget GC–MS have typically employed the extensive separation power of two-dimensional gas chromatography with specialized data processing.[11,12] The alignment of one-dimensional GC electron ionization (EI) data poses different challenges from that of LC because molecular ions are rarely dominant, and many common fragments are produced. The few efforts to jointly characterize chemicals in environmental samples using LC and GC–HRMS in tandem have relied on vendor software[13,14] that involves significantly different workflows across the platforms. Software platforms that integrate GC and LC workflows are available from the field of metabolomics,[15] but such approaches have not been widely applied to nontarget monitoring of environmental contaminants.

Even with advanced HRMS instrumentation and state-of-the-art workflows, confirming tentative compound identifications requires a substantial commitment of analyst time and resources to purchase or synthesize authentic standards. Moreover, toxicological profiles for

many of the compounds identified by these workflows may be incomplete or nonexistent, hampering hazard assessment. *In vitro* bioassays allow the relative hazards of different environmental samples to be assessed and support the prioritization of further compound identification. In the context of health hazards from wildfires, bioassay endpoints of concern include dioxin-like responses, endocrine disruption, and inflammation. Dioxin-like activity of chemicals is mediated by the aryl hydrocarbon (dioxin) receptor (AhR), a nuclear receptor which binds dioxins and related chemicals with high affinity and stimulates the expressions of a battery of genes, including cytochrome P4501A1 (CYP1A1).[16] Recombinant cell lines containing an AhR-responsive firefly luciferase reporter gene have been extensively utilized as a simple and sensitive bioassay for the detection and relative quantitation of dioxin-like chemicals, PAHs, and related AhR activators in diverse environmental extracts, including ash.[17–21] Similarly, the ability of environmental chemicals to modulate the activity of estrogen and androgen receptors (ER and AR, respectively), nuclear receptors that play a key role in regulating the expression of genes important in reproductive and other biological effects, have been linked to a variety of adverse endocrine disruption effects.[11,22,23] Recombinant cell lines containing ER- or AR-responsive luciferase reporter genes have been developed and utilized for the detection of activators and inhibitors of these receptor signaling pathways in the extracts of environmental matrices, including atmospheric particulate materials, and environmental contaminants such as PAHs.[19,21–24] AhR-, ER-, and AR-responsive cell lines were used to assess the ability of wildfire extracts to produce estrogenic, androgenic, and dioxin-like activities. A bioassay consisting of human U937-derived macrophages was used to test the potential activity of wildfire samples to induce inflammatory biomarkers which are relevant factors in mediating human health effects including lung injuries and cardiovascular diseases. The macrophage cell line used as a bioassay in this study is an important cell type providing a first line of defense in the innate immune response.[25] Macrophages have the unique ability to phagocytose cell debris and other materials. Further, they have been shown to produce inflammatory cytokines after treatment with chemicals generated by combustion.[26] Macrophages are also known to be critically involved in inflammatory diseases including lung injury and cardiovascular disease.[27,28]

The Tubbs fire, which burned over 36,000 acres in Napa and Sonoma counties (CA, USA) during October 2017, was the fourth deadliest and the second most destructive fire in state history, causing 22 deaths and destroying over 5000 structures.[1] As part of a larger effort to understand human health effects in the aftermath of this devastating fire, ash samples were collected from both burned residential areas and undeveloped background sites, and the extracts were analyzed using both LC– and GC–HRMS methods. The goals of the research were to: (i) demonstrate the application of integrated LC– and GC–HRMS workflows to identify unknowns in environmental samples, (ii) compare the organic compound composition of ash samples from developed and undeveloped areas to determine compounds unique to, or highly enriched in, urban/residential areas relative to undeveloped areas, (iii) use *in vitro* bioassays to assess the bioactivity of samples and to identify compounds potentially related to the bioactivity, and (iv) provide information needed to guide further research, monitoring, and hazard assessment in the aftermath of wildfires within developed areas.

MATERIALS AND METHODS

Ash Collection.

Five sample clusters, each containing three collection sites, were sampled within the perimeter of the Tubbs fire on November 1, 2017. Figure 1 can be referred to for a map of the collection locations and Table S1 for GPS coordinates. The clusters generally follow a north–south transect from upwind to downwind of the fire origin, which was located close to site TBS. Each ash sample is a composite from multiple points at a particular site; for sites with burned structures, subsamples were taken from multiple interior locations, a garage, and an exterior location. For sites that did not have a burned structure (all at locations designated by RLS), composite samples were prepared from subsamples collected at similar distances. The samples were stored in glass containers with Teflon-lined caps at –20 °C until extractions were performed.

Ash Extraction for Chemical Analysis.

The collected ash samples were sieved (<600 μm), and subsamples were extracted separately for chemical and bioassay analyses. For chemical analysis, 100 mg ash samples were extracted with 3 mL of hexane/acetone (3:1 v/v) under sonication for 15 min. The supernatant was transferred to an empty test tube, and the samples were extracted again with 3 mL of acetone (100%) under sonication for 15 min. The supernatant was combined with the hexane/acetone extract. Each combined extract was filtered through a 0.2 μm polytetrafluoroethylene (PTFE) filter and evaporated to 1 mL. The extract was then split evenly into a GC fraction and a LC fraction. The GC fraction has a final volume of 0.5 mL and was spiked with an internal standard (4,4′-dibromooctafluorobiphenyl). The LC fraction was solvent-exchanged to methanol, and water was added to achieve a final volume of 0.5 mL. A mixture of labeled internal standards was added (Table S2). The labeled internal standards, which elute across the full chromatogram, were used to correct for retention time variations during alignment and to check for differences in the matrix suppression. Across this set of extracts, no significant differences were observed in the abundance of internal standards (coefficients of variation 6.8–19.7%); so, no abundance or matrix suppression corrections were implemented. For the bioassays, subsamples (1 g) of sieved ash were extracted in the same manner—using 3 mL of hexane/acetone (3:1 v/v) followed by 3 mL of acetone (100%) under sonication for 15 min. The supernatants were combined, filtered through a 0.2 μm PTFE filter, and evaporated to 0.1 mL. The extract was solvent-exchanged to dimethyl sulfoxide (DMSO) with a final volume of 0.5 mL and transferred to the laboratories that performed the bioassays described below.

GC–QTOF-MS Acquisition and Target Analysis.

Compounds in the GC fractions were separated using an Agilent 7890B gas chromatograph, and mass spectra were acquired using a 7200B quadrupole-time-of-flight mass spectrometry (GCQTOF-MS) instrument. An Agilent HP-5MS Ultra Inert (30 m × 0.25 mm × 0.25 μm) column was used, and the spectra were acquired in EI mode. Each acquisition was approximately 78 min with a linear temperature gradient from 35 to 325 °C for the analysis of a wide range of chemicals. The acquired data files were imported into Agilent MassHunter Quantitative Analysis (B.09) for the quantification of target compounds—17

PAHs and 5 dioxins. The most abundant ion was used as a quantifier, and two additional ions were used as qualifiers. The exact mass window for quantitation was ±25 ppm, but all compounds detected exhibited errors under 10 ppm. A 13-point calibration curve, ranging from 0.1 to 1000 ng/mL, was used to calculate the concentrations of PAHs and dioxins in extracts.

LC–QTOF-MS Acquisition.

The LC fractions were analyzed in triplicate injections on an Agilent 6530 liquid chromatograph quadrupole-time-of-flight mass spectrometer with an Agilent ZORBAX Eclipse Plus C18 column (2.5 × 100 mm × 1.8 μm). Both positive and negative ESI (ESI^+/ESI^-) modes were used with the following mobile phases: for ESI^+, (A) ultrapure water plus 0.1% formic acid and (B) acetonitrile plus 0.1% formic acid; for ESI^-, (A) ultrapure water plus 1 mM ammonium fluoride and (B) acetonitrile. The injection volume was 10 μL. Acquisition was done in full scan mode with an acquisition rate of 4 spectra/s. Features with statistically significant ($p < 0.05$) Spearman's rank-order correlation coefficients between full scan MS ion abundances and one or more of the *in vitro* bioassays (described below) were selected for targeted MS/MS (tMSMS) experiments. LC fractions of selected samples with high ion abundances of the selected features were acquired in both ESI^+ and ESI^- using the same mobile phases used during the full scan MS acquisition. The injection volume was 5 μL. Only the target list of precursor ions was fragmented within the retention time window (0.4 min). The acquisition rate was 4 spectra/s with a mass range of 30 to 1050 *m/z*.

Nontarget Chemical Analysis.

Raw data from all GC– and LC–QTOF-MS experiments were first converted from the vendor format to the analysis base file format for further processing (Reifycs Analysis Base File Converter v. 4.0.0). All data were subsequently deconvoluted and aligned using MS-DIAL (v. 3.66 for GC data and v. 3.90 for LC data). A primary advantage of this workflow for the present application is the ability to handle both GC–EI and LC–ESI data using similar workflows.[15] The deconvoluted and aligned features in each data set were tentatively identified by searching against the NIST17 database (EI data) or an ionization mode-specific (ESI^+ or ESI^-) library created by combining the Agilent Water Contaminants, Pesticides, and Forensic Toxicology libraries. Parameter selection and workflow performance evaluation are described in detail in the Supporting Information. Samples with the highest abundances of high-priority LC compounds were reanalyzed using targeted MS/MS experiments, as described above; the data were deconvoluted using MSDIAL, and the results were exported to MS-FINDER (v. 3.24) to identify compounds against the databases and to conduct nontarget compound identification using *in silico* fragmentation approaches.[29]

Nuclear Receptor Cell Bioassays and Luciferase Analysis.

Sample extracts were evaluated for their ability to activate AhR-, ER-, and AR-dependent luciferase reporter gene expression in stably transfected mouse hepatoma (H1L6.1c3) and human breast carcinoma (VM7luc4E2 and T47DLucARE) cell lines, respectively.[22,30–32] The cell lines were grown and maintained in an alpha minimum essential medium (α-

MEM) containing 10% fetal bovine serum (FBS) in a humidified incubator at 37 °C with 5% CO_2. Prior to plating, endogenous estrogens were depleted from VM7Luc4E2 cells by growing cells in an estrogen-free medium (phenol red-free α-MEM containing 10% charcoal-stripped FBS and 1.9% L-glutamine) for 5 days.[30] All cell lines were plated into white, clear-bottomed 96-well tissue culture plates at a density of 75,000 cells/well and allowed to attach for 24 h prior to chemical treatments. The cells were incubated with the carrier solvent DMSO (1% final concentration), 1 nM 2,3,7,8-tetrachlorodibenzo-*p*-dioxin (TCDD) (for H1L6.1c3 cells), 1 nM 17β-estradiol (E2) (for VM7Luc4E2 cells), 10 μM testosterone (T) (for T47DLucARE cells), or an aliquot (1 μL) of the indicated extract (in DMSO) or test chemical in 100 μL medium for 24 h at 37 °C. For the analysis of AhR/ER antagonism, H1L6.1c3 or VM7Luc4E2 cells were incubated with 1 nM TCDD or 1 nM E2, respectively, in the absence or presence of the test extract for 24 h at 37 °C. All test extracts/chemicals and controls were analyzed in triplicate. After incubation, the cells were rinsed twice with phosphate-buffered saline and visually inspected under a microscope to evaluate the possible toxicity of sample extracts. Cell viability/cytotoxicity was assessed for all experiments using nuclear receptor cell lines using a scaled qualitative visual observation method previously approved by OECD[33] and ICCVAM[34] for the VM7Luc4E2 cells that scores viability on a scale of 1 (normal) to 4 (significant loss of viability). Cytotoxicity by this method is identified if cells exhibit any change in normal cell morphology or cell density (the latter resulting from cell death and/or cells detaching from the culture plate). As no cytotoxicity was observed in any cell line with any chemical or extract treatment, they were assigned a score of 1 (Normal Cell Morphology and Cell Density; for details, see Table 11–1 in ref 33). Cells were then lysed with 50 μL of Promega cell lysis buffer and shaken for 20 min at room temperature to allow complete cell lysis. Luciferase activity in each well was measured using an automated microplate luminometer (Orion, Berthold Detection Systems) in enhanced flash mode with the automatic injection of 50 μL of Promega stabilized luciferase reagent, as previously described in detail.[35] Luciferase activity (relative light units) of the solvent control (DMSO)-treated cells was subtracted from that of all treated cells to obtain the final induced luciferase activity of the test samples, and the values were then normalized to luciferase activity obtained with a maximal inducing concentration of the positive control chemical TCDD (1 nM), E2 (1 nM), or T (10 μM) (set at 100%).[30,32,33,42] Significant differences between the treated versus background (DMSO or method blank) samples were determined using Student's *t* test, with the statistical significance set at $p \leq 0.05$.

Ash Sample *In vitro* Exposure.

Cellular responses to ash sample extracts were quantified by measuring the gene expression levels including markers of toxicity and inflammatory responses detected by quantitative real-time reverse transcription-polymerase chain reaction (PCR). PCR analysis included cyclooxygenase-2 (COX-2) and interleukin 8 (IL-8) and the expression of cytochrome P450 1A1 (CYP1A1). Human U937 monocytic cells were obtained from the American Tissue Culture Collection (Manassas, VA) and maintained in RPMI 1640 medium containing 10% FBS (GIBCO), 100 U penicillin, and 100 μg/mL streptomycin. Cell cultures were maintained at cell concentrations between 2×10^5 and 2×10^6 cells/mL. For differentiation into macrophages, 2.5×10^5 U937 cells per well were seeded into 12-well tissue culture

plates and treated with 12–0-tetradecanoyl-phorbol-13-acetate (3 μg/mL) and allowed to adhere for 48 h, as described in ref 26. For PCR analysis and cell viability test, the macrophages were exposed in triplicate by adding 1 μL/mL of solvent (negative control), 1 μL/mL of ash sample extract, or 1 nM TCDD (positive control) directly to the media for 24 h.

Real-Time PCR.

After treatment, the total RNA was isolated from U937-derived macrophages using an RNA isolation kit (ZymoResearch, Irvine, CA) according to the manufacturer's instructions. Synthesis of cDNA was performed as previously described.[26] The expression of the housekeeping gene β-actin and differentially expressed genes was analyzed via real-time PCR with a LightCycler Instrument (LC 480, Roche Diagnostics, Mannheim, Germany), using the SYBR Green PCR kit (Applied Biosystems). All PCR assays were performed in triplicate, and results were expressed as fold induction relative to β-actin. The intra-assay variability was <7%. Data were analyzed with the LightCycler analysis software. No significant cytotoxicity was observed using the trypan blue exclusion test of cell viability for the macrophage cells when treated with any of the ash extracts at the level of 1 μL extract to 1 mL medium (Figure S1).

Statistical Analysis.

Relationships between the chemical composition of the ash extracts and their bioassay responses were explored using two separate approaches. First, the Spearman rank-order correlation coefficients were computed between each bioassay response and feature abundances using each ionization mode, with the corresponding p values adjusted for multiple hypothesis testing using the Benjamini–Hochberg procedure. The second approach sought sets of tentatively identified compounds that jointly were most predictive of the bioassay outcomes using elastic net regression,[36] as implemented in the R package glmnet (version 4.0–2, R version 4.0.2), with a mixing parameter of $\alpha = 0.05$ and fivefold cross-validation.

RESULTS AND DISCUSSION

Effects of Extracts on Aryl Hydrocarbon, Estrogen, and Androgen Receptor Activity.

The ability of ash extracts to affect AhR-, ER-, and AR-dependent gene expression was determined using a series of recombinant cell lines containing receptor-responsive firefly luciferase reporter genes. These cells respond to receptor agonists/activators in a chemical-, time-, concentration-, and receptor-dependent manner, with the induction of luciferase gene expression.[18,30–32] Although the AhR-responsive reporter gene expression in H1L6.1c3 cells was relatively low for most ash extracts (Figure 2), all extracts, except for TBS1, induced luciferase activity to a level that was statistically significantly greater than the activity of the method blank ($p \leq 0.05$). Interestingly, relatively high levels of AhR agonist activity were found for extracts COF2, COF3, MWS2, MWS3, and RLS3, with RLS3 and COF2 stimulating luciferase activity to 83 and 99%, respectively, of that of a maximal inducing concentration of the positive control, TCDD (Figure 2). In contrast, although little or no ER- or AR-dependent induction of luciferase was observed with any extract, inhibition

of the reporter gene activity below that of the method blank was observed with several extracts (Figure 2). A significant decrease in luciferase activity in the ER-responsive cell line VM7luc4E2 below that observed with the method blank was observed with extracts MW2, MW3, and RLS3. This reduction in luciferase activity is typical for ER antagonists as there remains some background luciferase activity because of a small amount of estrogen present in the cells even after several days of growth in estrogen-free media.[32] Thus, extracts MW2, MW3, and RLS3 appear to contain ER antagonists. Interestingly, these three extracts also contain AhR agonist activity (Figure 2), and given that some AhR activators are known to be ER antagonists,[16,37,38] it is possible that AhR-active compounds in these extracts contribute to the observed antiestrogenic activity. In contrast, the COF2 extract stimulated maximal AhR-dependent gene induction, compared to TCDD, but this extract produced no inhibition of basal luciferase activity in VM7Luc4E2 cells, indicating that the AhR-active chemicals in this extract were not antiestrogenic. This diversity in response is not surprising given that differential gene regulation by AhR agonists has been previously observed.[39] A significant reduction in luciferase activity in AR-responsive T47DLucARE cells below that of the method blank was observed for extract RLS3, the same extract that inhibited luciferase activity in the ER-responsive VM7Luc4E2 cells and induced an AhR response in H1L6.1c3 cells. These results are consistent with the recently reported ability of chemicals to interact with and produce differential response in AhR, ER, and AR signal transduction.[40] Overall, sample RLS3 had the most distinctive pattern of cell bioassay responses, with AhR activity that was the second highest among all samples and ER and AR activity that was the lowest among all samples; each of these activity levels differed significantly from the method blanks on the respective assays. The ER and AR antagonist activity of RLS3 was further confirmed by demonstrating that the RLS3 extract inhibited the induction of luciferase activity by E2 (in VM7Luc4E2 cells) and T (in T47DLucARE cells) by 23 and 74%, respectively (Tables S18 and S19).

Effect of Extracts from Wildfire Ash Samples on the Expression of CYP1A1 and Inflammatory Markers IL-8 and COX-2.

The ash extract impacts on the macrophage mRNA expression levels are shown in Figure 2 for CYP1A1 (top panel) and IL-8 and COX-2 (bottom panel). LRK ash samples did not significantly change the expression of CYP1A1, IL-8, or COX-2 in macrophages. Samples collected at the MWS sites had a relatively small effect on the mRNA expression of CYP1A1, with the highest increase of 7.6-fold above control after treatment with MWS2. The sample collected from TBS2 induced the expression of CYP1A1 mRNA level by 4.5-fold compared to control, whereas TBS1 and TBS3 had no significant effects. The ash sample from COF1 led to a 4.9-fold increase of the CYP1A1 mRNA level. Samples of COF2 led to a significant increase of 46.3-fold and COF3 led to a 19.8-fold elevated level of CYP1A1 compared to control samples. The highest increase of the CYP1A1 mRNA expression was found after treatment with RLS3 (112-fold), followed by RLS2 (11.1-fold) and RLS1 (8.4-fold).

The expression of the inflammatory markers COX-2 and IL-8 was significantly affected after treatment with the sample extracts from COF and RLS. The highest increase, 7.7-fold above control, was found for IL-8 mRNA in macrophages treated with RLS3, followed by

a 5.4-fold increase after treatment with COF2 (Figure 2). Treatment with RLS1 and RLS2 led to a minor increase of IL-8 of about threefold above control. The expression of COX-2 was significantly induced only by RLS3 (4.1-fold) followed by COF2 (3.6-fold). The extract samples collected at LRK and TBS had no significant effects on the expression of IL-8 or COX-2.

Target PAH Concentrations.

The concentrations of 16 PAHs (or pairs of coeluting isomers) were quantified (Table S8). Limits of quantification were in the range of 25–50 ng/g ash for PAHs with fewer than five fused rings and in the range of 100–250 ng/g for the higher molecular weight compounds. Five PAHs exceeded the LOQ in at least one ash sample, with naphthalene exceeding the LOQ in 12/15 samples. Sample RLS3 had the highest concentration of all compounds that exceeded the LOQ, except for phenanthrene in COF2.

GC Electron Ionization Alignment Results.

The MS-DIAL alignment of the GC–EI data for method blanks, calibration standards, and ash samples yielded a total of 595 molecular features; 583 of these compounds were present in at least one ash sample (summary statistics in Table 1, full set of GC–EI alignment results are shown in Table S9). To ensure that the aligned features are meaningful descriptors of the wildfire ash, a signal-to-noise filter (average S/N > 10) and a blank filter (maximum ash sample/average blank > 5) were applied, reducing the number of aligned features to 407; tentative identifications against the NIST17 database using the parameters in Table S4 were returned for 350 of these features. The statistical analyses presented below rely on assessing the relationships between the feature abundance for aligned features and bioassay activity; consequently, it is important to examine whether the feature abundance (peak height) values for aligned nontarget features provide a reliable measure of compound concentration. To test this, the peak height produced by MS-DIAL for several target PAHs is plotted against the peak height produced for the same samples by the Agilent quantitative analysis program while generating the quantification results presented in Table S8. For the seven PAHs most frequently detected across the ash sample set, the relationship between the two independently generated height estimates was highly linear ($0.86 < R^2 < 0.999$) with slopes between 0.808 and 1.04, with an average of 0.925 (Figure S2). This suggests that the GC–EI workflow can successfully align, identify, and provide quantitative abundance estimates for compounds known to be present in these samples to within ±20%; this strengthens confidence when applying the workflow to unidentified features in the data set. Although this analysis confirms a linear relationship between concentration and ion abundance for the target compounds in Figure S2, responses for the nontarget compounds may not be within the linear range of the instrument; this is one of the reasons that Spearman’s rank-order correlation coefficients are preferred over Pearson’s correlation coefficients for this analysis.

LC Electrospray Alignment Results.

The MS-DIAL alignment of the LC data yielded 4037 features in ESI^+ and 1757 features in ESI^-. Applying a filter that requires a feature to be present in all three replicate injections of at least one sample and to be present in at least one of the ash samples reduces the number of features to 2743/1113 (ESI^+/ESI^-; Tables S10 and S11). The same blank and

S/N features applied to the GC–EI data were also applied to the LC–ESI data but did not significantly reduce the number of features. A much lower fraction of the aligned features in the LC data sets had tentative identifications against the mass spectral databases listed in the Materials and Methods section (972/2637 ESI^+ and 429/1051 ESI^-), which are less extensive than the NIST library, and all tentatively identified compounds were based only on formula matches (MS1) from the full scan data collected in this study using the parameters found in Table S6. This failure to identify compounds in the LC data is not surprising given that the ash represents the residues from high-temperature combustion, and the databases used for the identification are those often used to screen for anthropogenic contaminants in environmental media like water or house dust. The results suggest that few toxic compounds that may have been present in the homes prior to the fire were present at levels detectable by our workflows in the ash samples we analyzed.

Comparing Developed and Undeveloped Sites.

A key goal of this study was to determine whether the residual compounds in the ash following an intense wildfire in a residential area were significantly more toxic than those collected at the corresponding undeveloped sites. The samples collected from Robert Louis Stevenson State Park (RLS1, RLS2, and RLS3) were at the northern boundary of the Tubbs fire impacted area, and throughout the event, prevailing winds were toward the south/southwest. Settled ash from the RLS sites is therefore believed to have been derived primarily from burned vegetation, whereas the samples from the other 12 sampling locations, which were all located within the footprint of burned residential structures, are viewed as being impacted by the combustion of construction materials, furnishings, and other contents of the homes. We considered two ways of isolating compounds that resulted from the combustion of residential structures. First, we determined the number of features that were present in at least one of the residential ash samples but that were not detected in any of the samples from the undeveloped sites (RLS). The number of features unique to the developed sites was much lower for GC–EI (14; 3.4% of filtered and aligned features) than for either LC–ESI^+ (251; 10% of features) or LC–ESI^- (291; 28% of filtered aligned features). A second strategy employed to select compounds of household origin was to identify features with an average abundance that was significantly different from the average at the undeveloped sites. This strategy generally yielded more compounds identified as originating from structure fires, with a total of 95, 413, and 124 features for GC–EI, LC–ESI^+, and LC–ESI^-, respectively, representing from 12 to 23% of aligned and filtered features. Taken together, these findings indicate that less than a quarter of the compounds found in the ash from developed areas might plausibly be derived from household materials, whereas most of the compounds in the ash are similar in identity and abundance to those found in undeveloped areas impacted by wildfires.

Bioassay–Feature Correlation.

Two strategies were used to attempt to select aligned features from the three compositional data sets (EI, ESI^+, and ESI^-) that were statistically associated with the biological activity measured in whole samples using the six selected bioassays. In the first approach, Spearman’s rank-order correlation coefficient between the nontarget feature abundance and the bioassay activity was calculated, and a two-tailed test was conducted to identify features

correlated with the bioassay activity. The p values for the correlation coefficients were corrected using the Benjamini–Hochberg procedure. The number of features positively or negatively correlated ($p < 0.05$) with the activity observed for each bioassay is reported in Table 1, and full lists of the correlated compounds by alignment number (as listed in Tables S9–S11) are provided in Tables S14–S16. The second approach applied to isolate the aligned features related to the bioassay activity was to apply the elastic net regression procedure.[36] The elastic net procedure produced a smaller set of bioassay-related features, with a maximum of 15 features selected, and with 11 of the 18 bioassay/ionization mode combinations returning null results (i.e., the model identified by elastic net as the most predictive of bioassay activity did not include any features).

Table S14 includes tentative identifications for the GC–EI molecular features associated with the bioassay extract activity. It is important to note that these identifications are those automatically generated by the MS-DIAL algorithm, which in 22% of cases misidentified structural isomers, as noted in the workflow testing results in Table S5. A specific example of this is feature 542, which was selected by the elastic net procedure as related to CYP1A1 and IL-8 activity and was tentatively identified as 1,3,7,9-tetrachlorodibenzo-*p*-dioxin. This assignment is incorrect based on the alignment of this feature with our authentic standard of TCDD. Although the abundance of this feature is well below our limit of detection for the target compound (Table S8), the selection of this low-abundance feature, as related to cytochrome P450 activation, illustrates the sensitivity and the limitations of this workflow.

To assess the success of the approaches used to identify compounds with potential biological activity from the complex mixtures of the wildfire ash extracts, we examined chemical screening results from the TOX21 program for assays corresponding to our AhR assay (TOX21_AhR_LUC_Agonist) and ER assay (TOX21_ERa_LUC_VM7_Agonist) available from the US EPA CompTox Chemicals Dashboard (https://comptox.epa.gov/dashboard). Searches for the reported activity on these two assays were conducted for each of the tentatively identified compounds from the GC–EI dataset. For the 407 aligned features that passed the blank and S/N filters, assay results were available for 91 compounds. For the AhR assay, 15 compounds displayed agonist activity (3.7%), 76 did not have agonist activity, and the remaining 316 had not been tested (Table 2). For the ER assay, 16 compounds displayed agonist activity (3.9%), 75 did not have agonist activity, and the remaining 316 did not have an assay result. The fraction of compounds with AhR and ER agonist activity was at least 5 times higher (≥20%) among the compounds selected by the Spearman rank-order correlation and elastic net procedures (Table 2). These comparisons are still limited by the relatively poor compound coverage of the available assay results. In the case of the elastic net regression results for AhR activity, for example, three of the five compounds returned by the procedure had not been tested.

To expand the assay coverage of tentatively identified compounds, we referred to an in-house database of bioassay results (UC Davis database) containing 9832 compounds with AhR agonist activity. This database contains agonist compounds identified in a high-throughput screen of 324,858 compounds (PubChem AID2845), agonists from the Tox21AhR screen, unpublished results from laboratory screening of diverse chemicals, and AhR agonists identified from an extensive search of the published literature. As the

TOX21 results only contain 1988 compounds with AhR agonist activity, the UC Davis database significantly increased the number of known AhR agonists for tentatively identified compounds to be searched against. Examining the elastic net results in more detail, of the four compounds listed as AhR agonists, one of them, pentachlorophenol, was active in both TOX21 testing and the UC Davis database. Two others, anthracene and chrysene, were reported as agonists in our testing but had not been tested in the TOX21 program, whereas one compound, pyrene, was listed as not being an agonist in the TOX21 results but was listed as an agonist in the UC Davis database. The final compound returned by the elastic net procedure, 1,1′:2′,1″-terphenyl, 4′-phenyl-, was not present in either assay panel.

We selected five compounds that exhibited statistically significant positive Spearman's rank-order correlation coefficients between feature abundance and AhR activity or were identified by elastic net regression as related to AhR activity that had not previously been tested to analyze for their pure compound AhR activity (Table S17). All five of these tentatively identified compounds (4-acetoxy-benzaldehyde, 2-phenyl-naphthalene, 1,2,4-triphenyl benzene, pentachlorobenzene, and 2-(2-phenylethenyl)quinoline) exhibited statistically significant increases in AhR activation relative to controls ($p < 0.05$). Although 2-phenyl-naphthalene and 2-(2-phenylethenyl)quinoline were not potent activators (i.e., showed no significant effects at the lowest concentration tested), they were extremely efficacious, inducing AhR-dependent luciferase reporter gene activity in a concentration-dependent manner, reaching a value 1.4 and 2.6 times greater than the maximal induction response of TCDD, respectively, at the highest concentration tested (Table S17). Superinduction of AhR-dependent reporter gene expression in these and other cell lines has been previously reported[41–44] and can result via the interaction of the test chemical(s) with a variety of cellular signaling pathways and transcription factors to enhance reporter gene expression in these cells. Pentachlorobenzene was a moderately efficacious AhR activator inducing reporter gene expression to 44% of that of TCDD, and 4-acetoxy-benzaldehyde was a very weak AhR agonist, with a concentration of 100 μM, inducing AhR-dependent gene expression to only 6% of that of TCDD. Although 1,2,4-triphenyl benzene was a slightly more potent AhR agonist than the other chemicals at the lowest concentration, with 1 μM inducing AhR-dependent gene expression to 12% of that of TCDD, the agonist response declined with increasing concentration. The additional information from the UC Davis database and subsequent targeted AhR analysis improved the apparent success of the statistical procedures in isolating AhR agonists from the ash extracts, with 70.6% of the compounds with significant Spearman's rank-order correlation coefficients displaying AhR agonist activity and 100% of the compounds selected by the elastic net regression displaying activity (Table 2).

tMSMS data were successfully obtained for relatively few features detected via LC–HRMS with potential relationships to bioassay endpoints (25/276 ESI^+ and 51/223 ESI^-), and fewer of these could be successfully annotated with tentative structural information. This was largely because of the low abundance and/or poor fragmentation of the precursor ions. However, it is worth considering the success of the method in selected cases to inform future method development. Four compounds are examined further here, two returned by tMSMS in ESI^+ and two in ESI^-. In ESI^+, feature 243, which was negatively correlated with CYP1A1 and AhR activity and positively correlated with AR activity, returned

the top-ranked structure of 2-isopropyl-5-methylfuran and a second ranked structure of 2-butylfuran (Figure S4). Neither compound has been tested under the Tox21 program, but 2-butylfuran is predicted to be inactive toward the AR using multiple ToxCast models. The structurally similar compound 2-pentylfuran was found to be an AR antagonist in Tox21 testing (TOX21_AR_BLA_Antagonist_ratio). The second ESI^+ compound considered here is feature 2608, which was negatively correlated with COX2 activity and was identified as related to AR activity by the elastic net regression procedure. This feature was tentatively identified as a harmala alkaloid (Figure S4), a structure that is not available within the CompTox Chemicals Dashboard. No relevant bioactivity measurements could be found for this compound in PubChem, but harmaline has been shown to be an AhR agonist.[45] The first ESI^- example structure is feature 820, which was positively correlated with CYP1A1 and IL-8 activity and negatively correlated with AR activity (Table S16). This compound was tentatively identified as the diphenylether cyperine (2-(3-hydroxy-5-methylphenoxy)-5-methoxy-3-methylphenol; Figure S5). The compound does not have either Tox21 data or ToxCast predictions, and no relevant bioactivity was indicated in the PubChem record. The second ESI^- example is feature 1148, which was positively correlated with CYP1A1, IL-8, and COX-2 activity and negatively correlated with ER and AR activity (Table S16). This compound was tentatively identified as the retrochalcone licoagrochalcone B (Figure S5) and was not present in the CompTox Chemistry Dashboard. The PubChem record for the top two structures for feature 1148 did not indicate any relevant bioactivity. Overall, the nontarget LC–HRMS structure search was significantly less successful than the corresponding GC–HRMS search in the identification of compounds, either novel or expected, that exhibit the types of effects represented by the suite of bioassays applied in this study.

Implications and Future Directions.

The results reported here suggest that the coordinated application of nontarget chemical analysis using HRMS, whole extract testing using *in vitro* bioassay methods, and advanced statistical methods can successfully identify compounds with potential toxicological significance from complex environmental matrixes such as wildfire ash. Further advances are obviously possible with improved compound coverage in bioassay panels or using computational approaches to assess, for example, the nuclear receptor binding affinity of tentatively identified compounds without reported bioassay activity. The method presented here also presumes that bioactive compounds in these mixtures act in an additive manner, an assumption that is clearly not universally true; the interaction between nuclear receptor agonists and antagonists within samples provide an important exception that will be difficult or impossible to detect with the workflows reported here. Further work is required to develop methods to account for such interactions.

With respect to the wildfire ash samples in particular, even though a large number of nontarget compounds were present in ash samples from residential areas destroyed by the fires in comparison to those from burned wildland areas, these compounds did not appear to be responsible for the measured biological activity on the battery of six bioassays applied in this research. Combined with the discovery of very few anthropogenic xenobiotic compounds in the ash extracts, as opposed to the known combustion byproducts like PAHs,

this suggests that ash from residential areas destroyed by wildfires is not intrinsically more hazardous than the ash from similarly impacted wildland areas. This knowledge should be helpful in assessing post-wildfire risks to returning residents and construction crews and in better understanding the impacts of fire debris on other environmental compartments such as surface water.

Supplementary Material

Refer to Web version on PubMed Central for supplementary material.

ACKNOWLEDGMENTS

Research reported in this publication was supported by the National Institute of Environmental Health Science of the National Institutes of Health under award numbers P42 ES004699, R21 ES029693, and R01 ES029126. The content is solely the responsibility of the authors and does not necessarily represent the official views of the National Institutes of Health. The authors appreciate the laboratory assistance provided by Chris Alaimo, Annie Kirkwood, Guillemette Calderwood, and Berkley Anderson and programming assistance from Caleb Young.

REFERENCES

(1). California Department of Forestry and Fire Protection Top 20 Most Destructive California Wildfires. https://www.fire.ca.gov/statsevents/ (accessed Sept 25, 20).

(2). Beitel SC; Flahr LM; Hoppe-Jones C; Burgess JL; Littau SR; Gulotta J; Moore P; Wallentine D; Snyder SAAssessment of the toxicity of firefighter exposures using the PAH CALUX bioassay. Environ. Int. 2020, 135, 105207.

(3). Adetona AM; Kyle Martin W; Warren SH; Hanley NM; Adetona O; Zhang J; Simpson C; Paulsen M; Rathbun S; Wang J-S; DeMarini D; Naeher LPUrinary mutagenicity and other biomarkers of occupational smoke exposure of wildland firefighters and oxidative stress. Inhalation Toxicol. 2019, 31, 73–87.

(4). Keir JLA; Akhtar US; Matschke DMJ; Kirkham TL; Chan HM; Ayotte P; White PA; Blais JMElevated Exposures to Polycyclic Aromatic Hydrocarbons and Other Organic Mutagens in Ottawa Firefighters Participating in Emergency, On-Shift Fire Suppression. Environ. Sci. Technol. 2017, 51, 12745–12755. [PubMed: 29043785]

(5). García-Falcón MS; Soto-González B; Simal-Gándara J. Evolution of the concentrations of polycyclic aromatic hydrocarbons in burnt woodland soils. Environ. Sci. Technol. 2006, 40, 759–763. [PubMed: 16509315]

(6). Lemieux PM; Lutes CC; Santoianni DAEmissions of organic air toxics from open burning: a comprehensive review. Prog. Energy Combust. Sci. 2004, 30, 1–32.

(7). Moschet C; Wittmer I; Simovic J; Junghans M; Piazzoli A; Singer H; Stamm C; Leu C; Hollender J. How a Complete Pesticide Screening Changes the Assessment of Surface Water Quality. Environ. Sci. Technol. 2014, 48, 5423–5432. [PubMed: 24821647]

(8). Ruff M; Mueller MS; Loos M; Singer HPQuantitative target and systematic non-target analysis of polar organic micropollutants along the river Rhine using high-resolution massspectrometry – Identification of unknown sources and compounds. Water Res. 2015, 87, 145–154. [PubMed: 26402878]

(9). Helbling DE; Hollender J; Kohler H-PE; Singer H; Fenner K. High-Throughput Identification of Microbial Transformation Products of Organic Micropollutants. Environ. Sci. Technol. 2010, 44, 6621–6627. [PubMed: 20799730]

(10). Schymanski EL; Singer HP; Longrée P; Loos M; Ruff M; Stravs MA; Ripollés Vidal C; Hollender J. Strategies to Characterize Polar Organic Contamination in Wastewater: Exploring the Capability of High Resolution Mass Spectrometry. Environ. Sci. Technol. 2014, 48, 1811–1818. [PubMed: 24417318]

(11). Shaul NJ; Dodder NG; Aluwihare LI; Mackintosh SA; Maruya KA; Chivers SJ; Danil K; Weller DW; Hoh E. Nontargeted Biomonitoring of Halogenated Organic Compounds in Two Ecotypes

of Bottlenose Dolphins (Tursiops truncatus) from the Southern California Bight. Environ. Sci. Technol. 2015, 49, 1328–1338. [PubMed: 25526519]

(12). Megson D; Robson M; Jobst KJ; Helm PA; Reiner EJDetermination of Halogenated Flame Retardants Using Gas Chromatography with Atmospheric Pressure Chemical Ionization (APCI) and a High-Resolution Quadrupole Time-of-Flight Mass Spectrometer (HRqTOFMS). Anal. Chem. 2016, 88, 11406–11411. [PubMed: 27934115]

(13). Moschet C; Lew BM; Hasenbein S; Anumol T; Young TMLC- and GC-QTOF-MS as Complementary Tools for a Comprehensive Micropollutant Analysis in Aquatic Systems. Environ. Sci. Technol. 2017, 51, 1553–1561. [PubMed: 28026950]

(14). Moschet C; Anumol T; Lew BM; Bennett DH; Young TMHousehold Dust as a Repository of Chemical Accumulation: New Insights from a Comprehensive High-Resolution Mass Spectrometric Study. Environ. Sci. Technol. 2018, 52, 2878–2887. [PubMed: 29437387]

(15). Tsugawa H; Cajka T; Kind T; Ma Y; Higgins B; Ikeda K; Kanazawa M; VanderGheynst J; Fiehn O; Arita M. MS-DIAL: data-independent MS/MS deconvolution for comprehensive metabolome analysis. Nat. Methods2015, 12, 523–526. [PubMed: 25938372]

(16). Denison MS; Soshilov AA; He G; DeGroot DE; Zhao B. Exactly the Same but Different: Promiscuity and Diversity in the Molecular Mechanisms of Action of the Aryl Hydrocarbon (Dioxin) Receptor. Toxicol. Sci. 2011, 124, 1–22. [PubMed: 21908767]

(17). Bergknut M; Kucera A; Frech K; Andersson E; Engwall M; Rannug U; Koci V; Andersson PL; Haglund P; Tysklind M. Identification of potentially toxic compounds in complex extracts of environmental samples using gas chromatography-mass spectrometry and multivariate data analysis. Environ. Toxicol. Chem. 2007, 26, 208–217. [PubMed: 17713206]

(18). Denison M; Zhao B; Baston DS; Clark GC; Murata H; Han D-HRecombinant cell bioassay systems for the detection and relative quantitation of halogenated dioxins and related chemicals. Talanta2004, 63, 1123–1133. [PubMed: 18969542]

(19). Novák J; Vaculovič A; Klánová J; Giesy JP; Hilscherová K. Seasonal variation of endocrine disrupting potentials of pollutant mixtures associated with various size-fractions of inhalable air particulate matter. Environ. Pollut. 2020, 264, 114654.

(20). Sakai S.-i.; Takigami, H. Integrated biomonitoring of dioxin-like compounds for waste management and environment. Ind. Health2003, 41, 205–214. [PubMed: 12916751]

(21). Zajda K; Rak A; Ptak A; Gregoraszczuk ELCompounds of PAH mixtures dependent interaction between multiple signaling pathways in granulosa tumour cells. Toxicol. Lett. 2019, 310, 14–22. [PubMed: 30980910]

(22). Croes K; Van den Heuvel R; Van den Bril B; Staelens J; Denison MS; Van Langenhove K; Vandermarken T; Elskens M. Assessment of estrogenic and androgenic activity in PM10 air samples from an urban, industrial and rural area in Flanders (Belgium) using the CALUX bioassay. Environ. Res. 2016, 150, 66–72. [PubMed: 27257826]

(23). Novák J; Giesy JP; Klánová J; Hilscherová K. In vitro effects of pollutants from particulate and volatile fractions of air samples-day and night variability. Environ. Sci. Pollut. Res. 2013, 20, 6620–6627.

(24). Pencikova K; Ciganek M; Neca J; Illes P; Dvorak Z; Vondracek J; Machala M. Modulation of endocrine nuclear receptor activities by polyaromatic compounds present in fractionated extracts of diesel exhaust particles. Sci. Total Environ. 2019, 677, 626–636. [PubMed: 31071665]

(25). Aderem A; Underhill DMMechanisms of phagocytosis in macrophages. Annu. Rev. Immunol. 1999, 17, 593–623. [PubMed: 10358769]

(26). Vogel CFA; Sciullo E; Wong P; Kuzmicky P; Kado N; Matsumura F. Induction of proinflammatory cytokines and Creactive protein in human macrophage cell line U937 exposed to air pollution particulates. Environ. Health Perspect. 2005, 113, 1536–1541. [PubMed: 16263508]

(27). Laskin DL; Pendino KJMacrophages and inflammatory mediators in tissue injury. Annu. Rev. Pharmacol. Toxicol. 1995, 35, 655–677. [PubMed: 7598511]

(28). Williams JW; Giannarelli C; Rahman A; Randolph GJ; Kovacic JCMacrophage Biology, Classification, and Phenotype in Cardiovascular Disease: JACC Macrophage in CVD Series (Part 1). J. Am. Coll. Cardiol. 2018, 72, 2166–2180. [PubMed: 30360826]

(29). Tsugawa H; Kind T; Nakabayashi R; Yukihira D; Tanaka W; Cajka T; Saito K; Fiehn O; Arita M. Hydrogen Rearrangement Rules: Computational MS/MS Fragmentation and Structure Elucidation Using MS-FINDER Software. Anal. Chem. 2016, 88, 7946–7958. [PubMed: 27419259]

(30). Brennan JC; Bassal A; He G; Denison MSDevelopment of a recombinant human ovarian (BG1) cell line containing estrogen receptor alpha and beta for improved detection of estrogenic/antiestrogenic chemicals. Environ. Toxicol. Chem. 2016, 35, 91–100. [PubMed: 26139245]

(31). Han D; Nagy SR; Denison MSComparison of recombinant cell bioassays for the detection of Ah receptor agonists. Biofactors2004, 20, 11–22. [PubMed: 15096657]

(32). Rogers JM; Denison MSRecombinant cell bioassays for endocrine disruptors: Development of a stably transfected human ovarian cell line for the detection of estrogenic and anti-estrogenic chemicals. In vitro Mol. Toxicol. 2000, 13, 67–82.

(33). OECD Performance-Based Test Guideline for Stably Transfected Transactivation In vitro Assays to Detect Estrogen Receptor Agonists and Antagonists. 2016, https://www.oecd-ilibrary.org/environment/test-no-455-performance-based-test-guideline-forstably-transfected-transactivation-in-vitro-assays-to-detect-estrogenreceptor-agonists-and-antagonists_9789264265295-en.

(34). ICCVAM An In vitro Assay for Identifying Human Estrogen Receptor Agonist and Antagonist Activity of Chemicals. 2011; National Toxicology Program, National Institute of Environmental Health Science, NIH, https://ntp.niehs.nih.gov/iccvam/docs/endo_docs/erta-tmer/bg1lucer-ta-tmer-combined.pdf.

(35). He G; Zhao J; Brennan JC; Affatato AA; Zhao B; Rice RH; Denison MSCell-Based Assays for Identification of Aryl Hydrocarbon (Ah) Receptor Activators. In Optimization of Drug Discovery: In vitro Methods, 2nd ed.; Yan A, Caldwell GW, Eds.; Humana Press: New York, NY, 2013; pp 221–235.

(36). Zou H; Hastie T. Regularization and variable selection via the elastic net. J. Roy. Stat. Soc. B Stat. Methodol. 2005, 67, 301–320.

(37). Rogers JM; Denison MSAnalysis of the antiestrogenic activity of 2,3,7,8-tetrachlorodibenzo-p-dioxin in human ovarian carcinoma BG-1 cells. Mol. Pharmacol. 2002, 61, 1393–1403. [PubMed: 12021401]

(38). Swedenborg E; Pongratz I. AhR and ARNT modulate ER signaling. Toxicology2010, 268, 132–138. [PubMed: 19778576]

(39). Safe S; Jin U-H; Park H; Chapkin RS; Jayaraman A. Aryl Hydrocarbon Receptor (AHR) Ligands as Selective AHR Modulators (SAhRMs). Int. J. Mol. Sci. 2020, 21, 6654.

(40). Doan TQ; Connolly L; Igout A; Nott K; Muller M; Scrippo MIIn vitro profiling of the potential endocrine disrupting activities affecting steroid and aryl hydrocarbon receptors of compounds and mixtures prevalent in human drinking water resources. Chemosphere2020, 258, 127332.

(41). Baston DS; Denison MSConsiderations for potency equivalent calculations in the Ah receptor-based CALUX bioassay: Normalization of superinduction results for improved sample potency estimation. Talanta2011, 83, 1415–1421. [PubMed: 21238730]

(42). Long WP; Chen X; Perdew GHProtein kinase C modulates aryl hydrocarbon receptor nuclear translocator protein-mediated transactivation potential in a dimer context. J. Biol. Chem. 1999, 274, 12391–12400. [PubMed: 10212212]

(43). Ma Q. Induction and superinduction of 2,3,7,8-tetrachlorodibenzo-p-dioxin-inducible poly(ADP-ribose) polymerase: Role of the aryl hydrocarbon receptor/aryl hydrocarbon receptor nuclear translocator transcription activation domains and a labile transcription repressor. Arch. Biochem. Biophys. 2002, 404, 309–316. [PubMed: 12147270]

(44). Zhao B; Baston DS; Khan E; Sorrentino C; Denison MSEnhancing the response of CALUX and CAFLUX cell bioassays for quantitative detection of dioxin-like compounds. Sci. China: Chem. 2010, 53, 1010–1016. [PubMed: 21394221]

(45). El Gendy MAM; Soshilov AA; Denison MS; El-Kadi AOSHarmaline and harmalol inhibit the carcinogen-activating enzyme CYP1A1 via transcriptional and posttranslational mechanisms. Food Chem. Toxicol. 2012, 50, 353–362. [PubMed: 22037238]

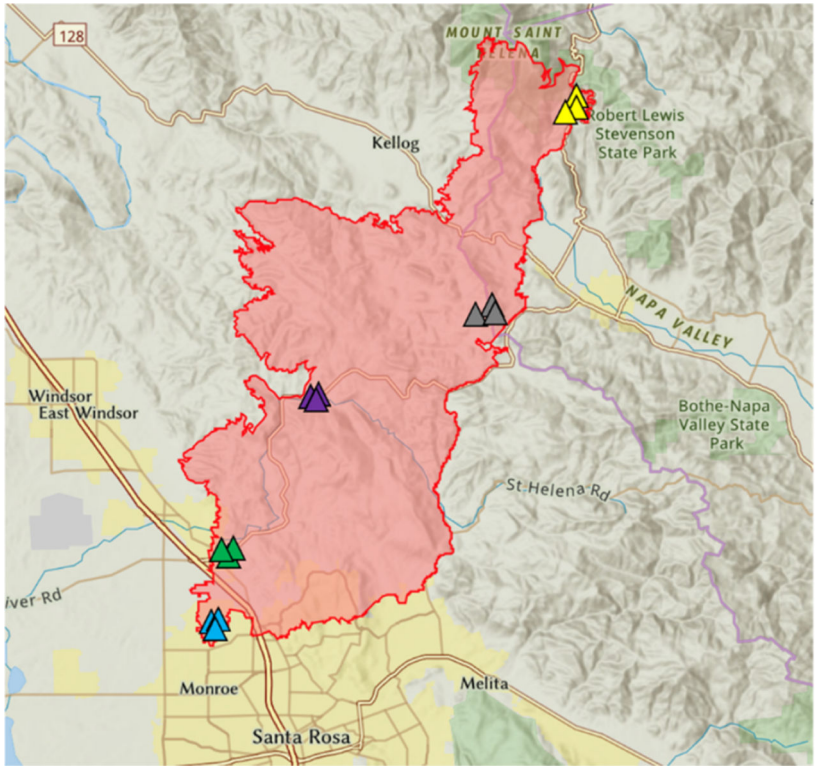

△	Robert Lewis Stevenson State Park (RLS)
△	Tubbs Lane (TBS)
△	Mark West Springs (MWS)
△	Larkfield Wikiup (LRK)
△	Coffey Park (COF)

Figure 1.
Extent of Tubbs fire and locations where samples were collected.

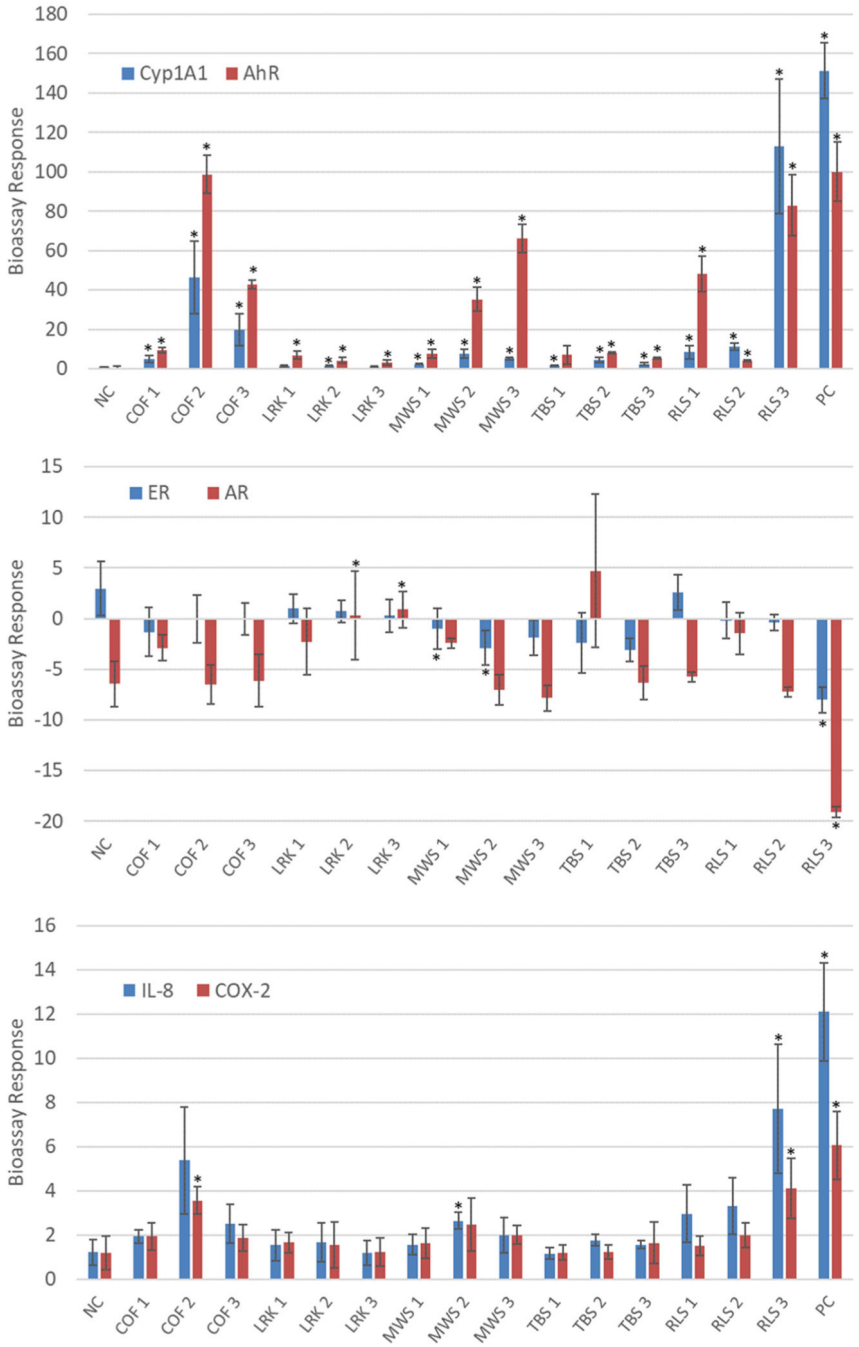

Figure 2.

Bioassay results for ash extracts. Bioassays include aryl hydrocarbon receptor (AhR) activity and cytochrome P450 (CYP1A1) mRNA expression (top panel), estrogen receptor α (ER) and AR activity (middle panel), and IL-8 and COX-2 mRNA expression (bottom panel). Values are expressed as the mean ± SD of at least triplicate analyses. * indicates significant difference from the method blank ($p < 0.05$). Bioassay responses are expressed as follows: AhR = % of 1 nM TCDD; ER = % of 1 nM estradiol; AR = % of 10 μM testosterone; CYP1A1, IL-8, COX-2 = fold change relative to control. NC = negative control (solvent

blank), PC = positive control, TCDD for AhR, CYP1A1, IL-8, COX-2. PC not shown for AR and ER to facilitate readability.

Table 1.

Summary of Molecular Feature Filtering Results and Numbers of Features with Statistically Significant ($p < 0.05$) Linear Correlations with Bioassay Endpoints

	GC–EI	LC–ESI$^+$	LC–ESI$^-$
aligned features in ash samples	583	4037	1757
after blank, S/N, and replication filters	407	2637	1051
CYP1A1-correlated (±)	33/11	54/32	58/8
IL-8-correlated (±)	34/5	80/23	137/6
COX-2-correlated (±)	22/1	14/35	16/5
AhR-correlated (±)	17/3	37/25	16/7
ER-correlated (±)	5/10	7/37	4/25
AR-correlated (±)	5/15	8/73	6/113
CYP1A1 elastic net	13	0	0
IL-8 elastic net	15	2	0
COX-2 elastic net	6	0	0
AhR elastic net	5	0	0
ER elastic net	0	4	0
AR elastic net	0	14	0
correlated with at least one bioassay	76	276	223
tentative ID among bioassay-correlated features	68	128	77
present in urban samples and absent from undeveloped samples	14	251	291
higher in urban samples than in undeveloped area ($p < 0.05$)	95	413	124

Table 2.

Comparison of Approaches for Selecting Molecular Features with Bioassay Activity

	confirmed AhR activity		ER activity
	TOX21 only	**TOX21 + UCD database + target tests**	**TOX21 only**
all tentatively identified features	15/407 (3.7%)	28/407 (6.9%)	16/407 (3.9%)
Spearman rank-correlated features	4/17 (23.5%)	12/17 (70.6%)	1/5 (20%)
elastic net regression-selected features	1/5 (20%)	5/5 (100%)	N/A